

The dispersion-managed Ginzburg–Landau equation and its application to femtosecond lasers

Gino Biondini

State University of New York at Buffalo, Department of Mathematics, Buffalo, NY 14260, USA

Received 7 February 2008, in final form 22 September 2008

Published 13 November 2008

Online at stacks.iop.org/Non/21/2849

Recommended by J Lega

Abstract

The complex Ginzburg–Landau equation has been used extensively to describe various nonequilibrium phenomena. In the context of lasers, it models the dynamics by averaging over the effects that take place inside the cavity. Pulses produced by Ti:sapphire femtosecond lasers, however, undergo significant changes in different parts of the cavity during each round-trip. The dynamics of such pulses is therefore not adequately described by an average model that does not take such changes into account. The purpose of this work is severalfold. We introduce the dispersion-managed Ginzburg–Landau equation (DMGLE) as an average model that describes the long-term dynamics of systems characterized by rapid variations of dispersion, nonlinearity and gain in a general setting, and we study the properties of the equation. We then explain how in particular the DMGLE arises for Ti:sapphire femtosecond lasers and we characterize its solutions. In particular, we show that, for moderate values of the gain/loss parameters, the solutions of the DMGLE are well approximated by those of the dispersion-managed nonlinear Schrödinger equation (DMNLSE), and the main effect of gain and loss dynamics is simply to select one among the one-parameter family of solutions of the DMNLSE.

PACS numbers: 42.65.Tg, 42.60.FC, 42.65.Re, 42.65.Sf

(Some figures in this article are in colour only in the electronic version)

1. Introduction

The complex Ginzburg–Landau equation (CGLE) is a universal model that governs the nonequilibrium dynamics of weakly nonlinear systems in the presence of gain, saturation, as well as linear and nonlinear dispersion, and describes a large variety of physical phenomena, from nonlinear waves to second-order phase transitions, superconductivity superfluidity, Bose–Einstein condensation, liquid crystals and strings in field theory [14, 21]. In particular, equations of the CGLE type have often been used as a model for the description of

mode-locked lasers [27, 28, 36, 39, 40, 52, 59]. The most well-known example in this context is referred to as the master equation of passive mode-locking [27, 36].

Lasers have a number of important scientific and technological applications, of course. In particular, the latest generation of Ti:sapphire femtosecond lasers [22, 65] could be used in spectroscopy, frequency metrology and optical atomic clocks [23, 31, 47, 62]. One of the features of these lasers is the presence of large variations of dispersion and nonlinearity inside the cavity [19]. The two phenomena are called, respectively, dispersion management and nonlinearity management by analogy with optical fibre communications. Because of these variations, another mathematical tool which has been recently used in studies of femtosecond lasers is the dispersion-managed nonlinear Schrödinger equation (DMNLSE), which is a universal model that describes the long-term dynamics of weakly nonlinear dispersive pulses subject to large, periodic variations of the nonlinear and/or dispersion coefficients [1, 24]. It should be clear, however, that the CGLE and DMNLSE are both inadequate descriptions of Ti:sapphire lasers. On the one hand, the CGLE is derived under the assumption that the pulse changes per round-trip inside the cavity are small, a condition which is grossly violated in femtosecond lasers. As a result, the CGLE cannot provide an accurate description of the dynamics of such lasers. On the other hand, gain/loss effects are obviously significant in *any* laser, so the DMNLSE cannot be a fully accurate description of a laser.

In this work we address both of the above issues. Starting from a multidimensional perturbed CGLE with time-dependent coefficients, we derive a new equation—which we call the dispersion-managed Ginzburg–Landau equation (DMGLE)—that describes the long-term dynamics of weakly nonlinear systems subject to rapidly varying dispersion, nonlinearity and gain/loss. We then study the properties of this equation and we use it to investigate the behaviour of dispersion-managed solitons in femtosecond lasers. The outline of this work is the following: in section 2 we obtain the DMGLE in a general setting as the equation which describes the average dynamics of systems governed by the CGLE with large and rapidly varying coefficients. In section 3 we then show how in particular the DMGLE arises in the description of Ti:sapphire femtosecond lasers. In section 4 we study the symmetries, rate equations and linear modes of the DMGLE, and in section 5 we discuss solitary-wave solutions and their properties. Section 6 concludes with some final remarks.

2. From the CGLE to the DMGLE

Here we obtain the DMGLE in a general setting as the equation which describes the long-time dynamics of multidimensional systems governed by the CGLE with large, time-dependent and rapidly varying coefficients. We start from a perturbed cubic CGLE in dimensionless form with time-dependent coefficients

$$i \frac{\partial q}{\partial t} + \frac{1}{2} p(t/t_a, t) \nabla_x^2 q + n(t/t_a, t) |q|^2 q = i g(t/t_a, t) q, \quad (2.1)$$

where $q = q(\mathbf{x}, t) \in \mathbb{C}$, $\mathbf{x} = (x_1, \dots, x_N) \in \mathbb{R}^N$, $t \in \mathbb{R}$, ∇_x^2 is the Laplacian operator, and the coefficients p and n are complex: $p(\cdot) = p_{\text{re}}(\cdot) + i p_{\text{im}}(\cdot)$, etc. In the context of mode-locked lasers, these quantities have the following physical interpretation:

- $p_{\text{re}}(t/t_a, t)$ quantifies chromatic dispersion,
- $p_{\text{im}}(t/t_a, t)$ quantifies spectral filtering or band-limited gain,
- $n_{\text{re}}(t/t_a, t)$ quantifies nonlinear interactions mediated by the Kerr effect,
- $n_{\text{im}}(t/t_a, t)$ quantifies gain saturation,
- $g_{\text{re}}(t/t_a, t)$ quantifies linear gain

(see section 3 for a more detailed discussion). Here t_a is a short temporal scale characteristic of the problem, which will be defined more precisely below. Without loss of generality, the function $g(t/t_a)$ can be taken to be real, since an imaginary component of $g(t/t_a)$ can always be eliminated by defining a rescaled field via the phase $\exp[i \int g_{\text{im}}(t/t_a) dt]$. But the same statement does not apply to $p(t/t_a)$ and $n(t/t_a)$, of course.

Solutions of (2.1) with complex coefficients have been extensively studied; e.g. see [12, 14] and references therein. These studies treat the standard CGLE, namely, the case in which all the coefficients are constant. Solutions of (2.1) with large, time-dependent and rapidly varying coefficients, on the other hand, can be very different from those of the standard CGLE, and characterizing their behaviour is a nontrivial task. Moreover, to the best of our knowledge, this problem has not been addressed in the literature, despite its theoretical and practical relevance. Our goal is precisely to elucidate the dynamics of such solutions. We do so by employing a multiple-scale analysis similar to that used to study optical fibre communication systems in the presence of dispersion management [1, 63].

Multiple scales expansion and the DMGLE. If the temporal variations of the coefficients in (2.1) are not too large, one can employ a standard multiple-scale perturbation expansion, as was done for the NLSE in [63]. The result is that, to leading-order, the pulse satisfies a CGLE with constant coefficients that are simply the averages of those appearing in (2.1). Higher-order terms then give corrections to this leading-order behaviour. (Of course different starting models can give rise to different scenarios, e.g. see [45, 55].) When the coefficients in (2.1) exhibit large temporal variations, however, the situation is not as simple, since the standard perturbation expansion breaks down, as it does for the NLSE [63]. It is this latter case that is of interest here. There are three key assumptions for our analysis:

- (i) All of the coefficients in (2.1) are periodic with respect to their first argument. That is, $p(\zeta + 1, t) = p(\zeta, t) \forall \zeta \in \mathbb{R}$ and similarly for $n(\cdot)$ and $g(\cdot)$.
- (ii) The coefficients in (2.1) are rapidly varying. That is, the dimensionless period is $t_a \ll 1$.
- (iii) The function $p(\cdot)$ can be decomposed into the sum of two terms, describing, respectively, large periodic zero-mean oscillations and an $O(1)$ residual. Namely,

$$p(t/t_a, t) = \frac{1}{t_a} \Delta p(t/t_a) + p_{\text{res}}(t/t_a, t), \quad (2.2a)$$

with

$$\int_0^{t_a} \Delta p(t/t_a) dt = 0. \quad (2.2b)$$

Note that both Δp and p_{res} can have both a real and an imaginary component. (Indeed, this will be the case in section 3.) Note also that the double time dependence of $p(\cdot)$, $n(\cdot)$ and $g(\cdot)$ in (2.1) allows one to capture cases in which the corresponding physical parameters have both a fast and a slowly varying component with respect to time. Even though the simplest case is when all of the coefficients average to a constant (as in optical fibre communications [1]), the more general situation does not introduce significant complications in the method.

With the above assumptions, we introduce the fast temporal scale $\zeta = t/t_a$ and look for solutions in the form

$$q(\mathbf{x}, \zeta, t) = q^{(0)}(\mathbf{x}, \zeta, t) + t_a q^{(1)}(\mathbf{x}, \zeta, t) + O(t_a^2). \quad (2.3)$$

It is convenient to denote by $\bar{f}(\mathbf{x}, t)$ the average of a function $f(\mathbf{x}, t/t_a, t)$ over one map period, namely:

$$\bar{f}(\mathbf{x}, t) = \int_0^1 f(\mathbf{x}, \zeta, t) d\zeta = \frac{1}{t_a} \int_0^{t_a} f(\mathbf{x}, t'/t_a, t) dt'. \quad (2.4)$$

We then substitute the ansatz (2.3) into the CGLE (2.1) and solve the resulting perturbation expansion following standard procedures. At leading order in the expansion we have the following linear problem:

$$i \frac{\partial q^{(0)}}{\partial \zeta} + \frac{1}{2} \Delta p(\zeta) \nabla_x^2 q^{(0)} = 0. \quad (2.5)$$

The solution of (2.5) is of course trivially obtained using Fourier transforms. We denote Fourier transforms by a circumflex accent throughout, with the transform pair defined as

$$\hat{f}(\mathbf{k}) = \mathcal{F}[f(\mathbf{x})] = \int e^{i\mathbf{k}\cdot\mathbf{x}} f(\mathbf{x}) (d\mathbf{x}), \quad (2.6a)$$

$$f(\mathbf{x}) = \mathcal{F}^{-1}[\hat{f}(\mathbf{k})] = \frac{1}{(2\pi)^N} \int e^{-i\mathbf{k}\cdot\mathbf{x}} \hat{f}(\mathbf{k}) (d\mathbf{k}), \quad (2.6b)$$

where $(d\mathbf{x}) = dx_1 \cdots dx_N$ is the volume element in \mathbb{R}^N . (Integrals are complete—meaning over all of \mathbb{R}^N —throughout this work unless otherwise noted.) With these conventions, the general solution of (2.5) is

$$\hat{q}^{(0)}(\mathbf{k}, \zeta, t) = \hat{\chi}(\mathbf{k}, \Xi(\zeta)) \hat{u}(\mathbf{k}, t), \quad \hat{\chi}(\mathbf{k}, \xi) = e^{-i\xi k^2/2}, \quad (2.7)$$

where $k^2 = \mathbf{k} \cdot \mathbf{k}$,

$$\Xi(\zeta) = \Xi_o + \int_0^\zeta \Delta p(\zeta') d\zeta' \quad (2.8)$$

and Ξ_o is an arbitrary integration constant. Equation (2.7) separates the fast dynamics of the pulse from the slow dynamics: the exponential factor in (2.7) accounts for the rapid ‘breathing’ (periodic compression/expansion) of the pulse, while the slowly varying envelope $\hat{u}(\mathbf{k}, t)$ encodes the information about the core pulse shape. Inverting the Fourier transforms we get the leading-order solution in the spatial domain,

$$q^{(0)}(\mathbf{x}, \zeta, t) = \chi(\mathbf{x}, \Xi(\zeta)) * u(\mathbf{x}, t), \quad \chi(\mathbf{x}, \xi) = \frac{e^{ix^2/2\xi}}{\sqrt{(2\pi i)^N \xi}}, \quad (2.9)$$

where $x^2 = \mathbf{x} \cdot \mathbf{x}$ and \sqrt{z} is taken on the principal branch (with $|\arg(z)| < \pi$), and where the asterisk denotes the convolution integral, defined as

$$(f * g)(\mathbf{x}) = \int f(\mathbf{x}') g(\mathbf{x} - \mathbf{x}') (d\mathbf{x}'), \quad (2.10)$$

Above and below we used the convolution theorem, stating that $\mathcal{F}^{-1}[\hat{f}\hat{g}] = f * g$ and $\mathcal{F}[fg] = \hat{f} * \hat{g} / (2\pi)^N$. Note that $\hat{\chi}(\mathbf{k}, 0) = 1$ and $\chi(\mathbf{x}, 0) = \delta(\mathbf{x})$, where $\delta(\mathbf{x})$ is the N -dimensional Dirac delta. Therefore, at those points ζ for which $\Xi(\zeta) = 0$, the solution $q^{(0)}(\mathbf{x}, \zeta, t)$ coincides with $u(\mathbf{x}, t)$. Note also that, since $\chi(\mathbf{x}, \xi)$ is even in \mathbf{x} , the parity of $q^{(0)}(\mathbf{x}, \cdot, \cdot)$ is determined by that of $u(\mathbf{x}, \cdot)$. That is, if $u(\mathbf{x}, t)$ is even with respect to \mathbf{x} , $q^{(0)}(\mathbf{x}, \zeta, t)$ is also even; vice versa, if $u(\mathbf{x}, t)$ is odd $q^{(0)}(\mathbf{x}, \zeta, t)$ is also odd.

The function $u(\mathbf{x}, t)$ is arbitrary at this stage, and as usual must be determined at higher order in the expansion. At $O(1)$ we have the following forced linear problem:

$$i \frac{\partial q^{(1)}}{\partial \zeta} + \frac{1}{2} \Delta p(\zeta) \nabla_x^2 q^{(1)} = - \left[i \frac{\partial q^{(0)}}{\partial t} + \frac{1}{2} p_{\text{res}}(\zeta, t) \nabla_x^2 q^{(0)} + n(\zeta, t) |q^{(0)}|^2 q^{(0)} - ig(\zeta, t) q^{(0)} \right]. \quad (2.11)$$

The solution of (2.11) can also be easily obtained using Fourier transforms. To avoid secularities, however, a Fredholm solvability condition must be satisfied (which as usual

expresses the orthogonality of the forcing to the solutions of the homogeneous problem). After tedious but straightforward algebra, this condition yield

$$i \frac{\partial u}{\partial t} + \frac{1}{2} \bar{p}(t) \nabla_x^2 u + \iint u_{(x+x')} u_{(x+x'')} u_{(x+x'+x'')}^* K_{(x' \cdot x'')}(\mathbf{d}\mathbf{x}')(\mathbf{d}\mathbf{x}'') = i \bar{g}(t) u, \tag{2.12}$$

or, equivalently, in the Fourier domain,

$$i \frac{\partial \hat{u}}{\partial t} - \frac{1}{2} \bar{p}(t) k^2 \hat{u} + \iint \hat{u}_{(k+k')} \hat{u}_{(k+k'')} \hat{u}_{(k+k'+k'')}^* \hat{K}_{(k' \cdot k'')}(\mathbf{d}\mathbf{k}')(\mathbf{d}\mathbf{k}'') = i \bar{g}(t) \hat{u}, \tag{2.13}$$

where for brevity we have introduced the shorthand notation $u_{(x)} = u(\mathbf{x}, t)$ and $\hat{u}_{(k)} = \hat{u}(\mathbf{k}, t)$. (That is, subscripts in parentheses denote functional dependence, *not* partial differentiation.) The superscript $*$ denotes complex conjugation throughout, and the integration kernels (which are in general complex and time-dependent) are given by

$$\hat{K}(\xi, t) = \frac{1}{(2\pi)^{2N}} \int_0^1 n(\zeta, t) e^{i\Xi(\zeta)\xi} d\zeta \tag{2.14a}$$

and

$$K(\mathbf{x}' \cdot \mathbf{x}'', t) = (2\pi)^{2N} \mathcal{F}^{-1}[\hat{K}(\mathbf{k}' \cdot \mathbf{k}'', t)]. \tag{2.14b}$$

(Again, a straightforward calculation shows that, as in the one-dimensional DMNLSE [1], $K(\cdot, t)$ depends only on the dot product $\mathbf{x}' \cdot \mathbf{x}''$, not on \mathbf{x}' and \mathbf{x}'' separately. Note also that $\bar{p}(t) = \bar{p}_{\text{res}}(t)$.) We refer to (2.12) (or equivalently (2.13)) as the dispersion-managed Ginzburg–Landau equation or DMGLE.

Remarks. Several comments are now in order:

- If $\Delta p(\zeta) = 0$, then choosing $\Xi_o = 0$ one has $\Xi(\zeta) = 0$, which implies $\hat{K}(\xi, t) = 1/(2\pi)^{2N}$ and $K(\mathbf{x}' \cdot \mathbf{x}'', t) = \delta(\mathbf{x}' - \mathbf{x}'')$. Then (2.12) and (2.13) reduce to the usual CGLE with constant coefficients written in the spatial and Fourier domains.
- If $p_{\text{im}}(\zeta, t) = n_{\text{im}}(\zeta, t) = 0$, equation (2.12) reduces to the multidimensional extension of DMNLSE [1, 24], perturbed by the addition of linear gain and loss when $\bar{g}(t) \neq 0$. Then, if $\Delta p(\zeta) = 0$, equation (2.12) further reduces to the NLSE with constant coefficients, again possibly with gain and loss.
- Since the NLSE, the CGLE and the DMNLSE arise in many different physical situations, one can expect that the DMGLE will also have a wide range of applicability. Indeed, the above formulation is fairly general, and it allows one to study a variety of different scenarios, including spectral filtering and nonlinear loss and gain.
- Equations of NLS type or CGLE type with nonlocal nonlinearities arise in various physical situations. In particular, apart from optical fibre communications, they also appear in water waves, in which case they are known to be integrable [53].
- Like the DMNLSE (its counterpart for conservative systems), the DMGLE is a reduced model that retains the essential features of dispersion-managed systems while bypassing the complicated dynamics that take place within each period. As such, it should prove to be a useful model to investigate the long-time behaviour of nonconservative dispersion-managed systems, like the DMNLSE did for conservative ones.
- Since $q(x, \zeta_*, t) = u(x, t)$ whenever $\Xi(\zeta_*) = 0$, the value of Ξ_o simply dictates at which points inside the map the full solution of (2.1) coincides with its core pulse shape. At the same time, however, the choice of Ξ_o appears in $\hat{K}(\xi, t)$ and its transform, and therefore can sometimes be exploited to make them simpler. (For example, the corresponding kernels for the DMNLSE in the lossless case can be made real [1].)

- If $n(\zeta, t) \neq \text{const}$, the kernels $\hat{K}(\xi, t)$ and $K(\xi, t)$ can have a nonzero imaginary part even when $\Delta p_{\text{im}}(\zeta, t) = 0$. Indeed, this is the case in optical fibre communication systems with loss compensated by periodically spaced amplifiers, when one takes into account that the effective nonlinear coefficient in the NLSE is distance dependent due to the periodic power variations originated by the loss/amplification cycle.
- A multiple-scale averaging similar to the one described above can also be performed for the quintic Ginzburg–Landau equation. The result of such an averaging is that the quintic term in the original equation produces a quintic term in the DMGLE with a four-dimensional convolution integral and a corresponding integration kernel. Such a situation will not be considered here, however.

Finally, we reiterate that $\Delta p(\zeta)$ need not be real for the purposes of the multiple-scale expansion: the derivation applies without change when $\Delta p_{\text{im}}(\zeta) \neq 0$. Of course, some of the conclusions are different: $\Xi(\zeta)$ acquires an imaginary part, and this has two main consequences: (i) it leads to a periodic amplification/suppression of high-wavenumber components in the fast dynamics; (ii) it leads to different kernels in the DMGLE. While the first of these consequences can be considered to be minor (since it has no effect on the long-term behaviour of solutions), the second can in principle produce different and interesting phenomena.

3. The DMGLE in femtosecond lasers

We now discuss how the DMGLE appears in the description of Ti : sapphire lasers. Figure 1 shows a diagram of a typical experimental setup. The system consists of a continuous-wave (CW) pump, a titanium-doped sapphire crystal and a set of prisms and/or mirrors. The crystal, which constitutes the nonlinear medium, is characterized by a Kerr-type nonlinear response as well as by gain and gain saturation, and has a large normal group velocity dispersion. (That is, for CW waves whose electric field is written as $\text{Re}(E e^{ikz - \omega t})$, where $k(\omega)$ represents the linear dispersion relation, it is $k'' = \partial^2 k / \partial \omega^2 > 0$.) The prisms and mirrors, on the other hand, are especially designed to have a large anomalous dispersion to compensate that of the crystal. The output of such a system is a periodic stream of optical pulses with a typical duration of about 10 fs, a spectrum typically centred at 830 and 70 nm wide, and with a typical repetition rate of 90 MHz (e.g. see [31]).

Laser model. The evolution of a quasi-monochromatic optical pulse in a Kerr-type medium is usually well described by the NLSE, possibly with varying coefficients [10, 19, 57]. To accurately capture the behaviour of pulses in a laser, however, it is obviously necessary take into account the gain and loss dynamics [19, 46]. In Ti : sapphire lasers, the gain dynamics (including linear gain and gain saturation) takes place inside the crystal, while the losses are concentrated in the reflecting mirror(s) and the output coupler. Since the precise dependence of the gain on the amplitude is complicated and in general not known in closed form, one is forced to approximate. This is typically done by characterizing the response of the nonlinear medium via two main parameters: the small signal gain, G_{ss} (namely, the gain experienced by signals of small amplitude) and the saturated gain, G_{sat} (namely, the gain experienced by signals of large amplitude). Of these two parameters, G_{sat} can be obtained indirectly, because, for each system configuration, it must compensate exactly the total losses per cavity round-trip. The value of G_{ss} , however, is hard to characterize theoretically or experimentally. Note that the value of G_{sat} depends on the specific system configuration, most notably on the pump power. Note also that gain relaxation is also present, but occurs over much slower temporal

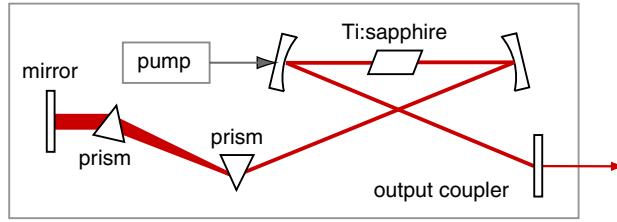


Figure 1. Schematic diagram of a prototypical Ti : sapphire femtosecond laser. See text for a detailed description.

scales than those of a single optical pulse. Since we are interested in the behaviour of pulses near steady state, this difference in the time scales is not a concern.

The gain dynamics is typically approximated by choosing a heuristic gain response function that interpolates between the small signal gain at low powers and the saturated gain at high powers. In particular, it was shown that choosing a Lorentzian-shape function yields a good approximation for the gain saturation (e.g. see [19, 27]). Let $E(Z, T)$ be the slowly varying envelope of the electric field, $Z = z_{\text{lab}}$ is the physical propagation distance and $T = t_{\text{lab}} - z_{\text{lab}}/v_g$ is the retarded time (that is, the time in a reference frame that moves with the group velocity $v_g = 1/k'(\omega)$ of the pulse). Neglecting all other effects for the moment, the combination of linear gain and gain saturation yields the following equation for the evolution of the electric field envelope inside the Ti : sapphire crystal:

$$\frac{\partial E}{\partial Z} = \frac{G_{\text{ss}}}{1 + |E/E_o|^2} E, \tag{3.1}$$

where E_o represents some appropriate reference amplitude. As in [35], we now expand the fraction $1/(1 + |E/E_o|^2)$ in Taylor series near $E = 0$. Retaining terms up to next-to-leading order, the right-hand side of (3.1) is then replaced by $G_{\text{ss}}(1 - |E|^2/|E_o|^2) E$.

Assuming that the gain spectrum does not change appreciably with the pump power over the operating range of the laser (which is a good approximation in Ti : sapphire lasers), one can neglect the second derivative of the cubic term when reinstating the time dependence. Then, recalling that the gain dynamics is confined to the crystal and combining the gain dynamics with the dispersive and nonlinear effects and the loss arising of the mirrors yields the following CGLE in dimensional form with distance-dependent coefficients:

$$i \frac{\partial E}{\partial Z} - \frac{1}{2} (k''(Z) - i\beta(Z)) \frac{\partial^2 E}{\partial T^2} + (\gamma(Z) + iG_{\text{nl}}(Z)) |E|^2 E = iG_o(Z) E, \tag{3.2}$$

where $k''(Z)$ and $\gamma(Z)$ are, respectively, the dispersion coefficient and the nonlinear coefficient, while $\beta(Z)$ quantifies band-limited gain.

The coefficients in (3.2) are conveniently parametrized by introducing the ‘indicator’ function $I(Z)$, which equals 1 for values of Z corresponding to locations inside the Ti : sapphire crystal and 0 otherwise. The coefficients in (3.2) can then be written as

$$k''(Z) = k''_{\text{Ti:s}} I(Z) + k''_{\text{dcm}} (1 - I(Z)), \tag{3.3a}$$

$$\beta(Z) = \beta_{\text{Ti:s}} I(Z), \quad \gamma(Z) = \gamma_{\text{Ti:s}} I(Z), \tag{3.3b}$$

$$G_o(Z) = G_{\text{ss}} I(Z) + G_{\text{dcm}} (1 - I(Z)), \quad G_{\text{nl}}(Z) = \frac{G_{\text{ss}} - G_{\text{sat}}}{|E_o|^2} I(Z), \tag{3.3c}$$

where the constants $k''_{\text{Ti:s}}, \gamma_{\text{Ti:s}} > 0$ are the dispersion and nonlinear coefficient of the Ti : sapphire crystal; $k''_{\text{dcm}} < 0$ quantifies the dispersion of the mirrors, prisms and output

coupler, as well as that of the air (which is experienced during the free-space propagation of the pulse in the cavity), and $G_{\text{dem}} < 0$ does the same for the loss. Note that, as written, (3.3a) and (3.3c) model the dispersion compensation and linear loss as taking place uniformly over the whole length of the cavity not occupied by the Ti:sapphire crystal. This is obviously not the case. Nonetheless, for the purposes of the averaging it is immaterial whether these effects occur at discrete locations or whether they are distributed, because all the processes occurring outside the crystal are linear.

Nondimensionalization and the DMGLE. Next we proceed to nondimensionalize (3.2). This requires more care than is necessary for the NLSE or the CGLE, because the dispersive effects are distance dependent. It also requires more care than is necessary for the DMNLSE, because the nonlinear effects are also distance dependent here.

Let $x = (t_{\text{lab}} - z_{\text{lab}}/v_g)/t_*$ and $t = z_{\text{lab}}/z_*$ be, respectively, the dimensionless retarded time and the dimensionless propagation distance, where z_* is a typical distance (defined below) and t_* is a typical time scale (e.g. the pulse duration). Also, let $q = E/E_*$ be the dimensionless slowly varying complex envelope of the electric field, where $P_* = |E_*|^2$ is a typical pulse power. Taking into account the fact that nonlinearity only acts inside the crystal, we then set $z_* = (L_{\text{Ti:s}}/L_a) z_{\text{NL}}$, where $L_{\text{Ti:s}}$ is the length of the Ti:sapphire crystal, L_a is the total length of the cavity and $z_{\text{NL}} = 1/(\gamma_{\text{Ti:s}} P_*)$ is the distance at which nonlinear effects become relevant. These changes of dependent and independent variables, transform (3.2) into the one-dimensional version of (2.1), with

$$p(\zeta) = d(\zeta) - ib(\zeta), \quad d(\zeta) = -k''(\zeta)/k_*'', \quad b(\zeta) = \bar{b} I(\zeta), \quad (3.4a)$$

$$n(\zeta) = (1 + i\bar{c}) I(\zeta)/\bar{I}, \quad g(\zeta) = G_o(\zeta) z_* \quad (3.4b)$$

(with a slight abuse of notation, where $\zeta = t/t_a$ as before, and where $k_*'' = t_*^2/z_*$, $\bar{b} = \beta_{\text{Ti:s}} \bar{I}/k_*''$ and $\bar{c} = (G_{\text{ss}} - G_{\text{sat}})/(\gamma_{\text{Ti:s}} |E_o|^2)$. (Note that $t_a = L_a/z_*$ and $\bar{I} = L_{\text{Ti:s}}/L_a$.) Without repeating the perturbation expansion of section 2, we can then apply its results to conclude that, to leading order, the dimensionless slowly varying envelope of the electric field is given by

$$q(x, t) = \mathcal{F}^{-1}[\hat{u}(k, t) e^{i\Xi(t/t_a)k^2/2}] \quad (3.5)$$

with

$$\Xi(\zeta) = \int_0^\zeta [d(\zeta') - \bar{d} - i(b(\zeta') - \bar{b})] d\zeta', \quad (3.6)$$

and where the slowly varying core $u(x, t) = \mathcal{F}^{-1}[\hat{u}(k, t)]$ solves the following DMGLE:

$$i \frac{\partial u}{\partial t} + \frac{1}{2}(\bar{d} - i\bar{b}) \frac{\partial^2 u}{\partial x^2} + (1 + i\bar{c}) \iint u_{(x+x')} u_{(x+x'')} u_{(x+x'+x'')}^* R_{(x'x'')} dx' dx'' = i\bar{g} u, \quad (3.7)$$

with $\bar{b}, \bar{c}, \bar{d}, \bar{g} \in \mathbb{R}$, and

$$R(x'x'') = \iint e^{-ik'x' - ik''x''} r(k'k'') dk' dk'', \quad (3.8a)$$

with

$$r(\xi) = \frac{1}{(2\pi)^2 \bar{I}} \int_0^1 e^{i\Xi(\zeta)\xi} I(\zeta) d\zeta. \quad (3.8b)$$

If $p(\zeta) \in \mathbb{R}$ (i.e. $b(\zeta) = 0$), it is $r^*(\xi) = r(-\xi)$ and $R^*(\xi) = R(-\xi)$. When $\bar{b} = \bar{c} = \bar{g} = 0$, (3.7) reduces to the DMNLSE derived in [1, 6].

The multiple-scale expansion is of course formally justified only when the expansion parameter t_a is small. Nonetheless, the DMNLSE—obtained under the same assumptions by neglecting the gain and loss dynamics—has been shown to provide a good qualitative (and in some cases even quantitative) description of the actual behaviour of pulses in Ti : sapphire femtosecond lasers even for system configurations where $t_a = O(1)$ [57]. One therefore expects that the DMGLE will also be a good model even in those situations.

As in section 2, the coefficients \bar{b} , \bar{c} , \bar{d} and \bar{g} could also depend on the evolution variable t . Such situations occur when the average dispersion, gain and gain saturation exhibit variations over slower temporal scales compared with the characteristic duration of the pulses in the cavity. Note also that the average dispersion depends on the details of the Kerr-lens process in the crystal, on the mirrors, the prisms and on the total cavity length. If $\bar{d} = \text{const}$, one can make its value unity by choosing $t_*^2 = \bar{k}'' z_*$. However, the general form is convenient if one wants to compare systems having different values of average dispersion (as in [57]), since in this case one can do so within the framework of a single DGMLE, without having to go back to the CGLE and choose different normalizations for each case.

Two-step maps. For the piecewise-constant two-step maps defined by (3.3a)–(3.3c), the kernels $r(\xi)$ and $R(\xi)$ in (3.7) can be computed explicitly and assume a very simple form. Taking the origin of the map at the output coupler, we have

$$I(\zeta) = \begin{cases} 0 & \zeta \in [0, \theta/2) \cup [1-\theta/2, 1), \\ 1 & \zeta \in [\theta/2, 1-\theta/2), \end{cases} \quad (3.9)$$

where $0 < \theta < 1$ represents the fraction of the cavity length not occupied by the Ti : sapphire crystal. This yields $\bar{I} = 1 - \theta$. Recalling that the linear effects acting on the pulse can be distributed throughout the portion of the cavity not occupied by the crystal, we then parametrize the zero-mean part of the dispersion as [1, 57]

$$\Delta d(\zeta) = \begin{cases} s/2\theta & \zeta \in [0, \theta/2) \cup [1-\theta/2, 1), \\ -s/[2(1-\theta)] & \zeta \in [\theta/2, 1-\theta/2), \end{cases} \quad (3.10)$$

where the map strength parameter s quantifies the L_1 -norm of $\Delta d(\zeta)$, as discussed in section 4. (This definition differs from the previous one [1, 57] by a factor 4.) Then

$$\Xi(\zeta) = \begin{cases} \Xi_+ \zeta & \zeta \in [0, \theta/2), \\ \Xi_-(\zeta - 1/2) & \zeta \in [\theta/2, 1-\theta/2), \\ \Xi_+(\zeta - 1) & \zeta \in [1-\theta/2, 1), \end{cases} \quad (3.11)$$

where $\Xi_+ = 2(s + ib_o)/\theta$ and $\Xi_- = -2(s + ib_o)/(1 - \theta)$, and with $b_o = \bar{b}\theta t_a/2$. After some straightforward calculations, one then obtains the kernels as

$$r(\xi) = \frac{1}{(2\pi)^2} \text{sinc}[(s + 2ib_o)\xi/4], \quad (3.12a)$$

$$R(\xi) = \frac{2}{\pi(s + ib_o)} \text{ci}[4\xi/(s + ib_o)], \quad (3.12b)$$

where $\text{sinc}(y) = (\sin y)/y$ and $\text{ci}(y) = \int_y^\infty \cos t dt/t$ is the cosine integral. The functional form of both kernels is identical to that of the DMNLSE. (The kernel in [57] differs by (3.12a) by an overall multiplicative constant due to the different choice of normalizations.) In the DMGLE, however, the kernels $r(\xi)$ and $R(\xi)$ appear multiplied by the complex factor $1+i\bar{c}$, which has important consequences on the equation (as we show in section 4) and on its solutions (as we show in section 5). Note that when $\bar{b} = 0$ both kernels are real, as for the DMNLSE

without linear gain and loss [1], and the specific details of the functions $\Delta d(t)$ and $I(t)$ do not affect the DMGLE nor its kernels. For this class of systems the DMGLE is a universal equation, in that it provides a unified description for the dynamics of different systems (such as the NLSE, CGLE and DMNLSE).

4. Symmetries, rate equations and linear modes

We now look at the properties of the DMGLE. For simplicity, in the remainder of this work we will restrict our attention to the form of the DMGLE that appears in femtosecond lasers, and to the case in which the coefficients \bar{b} , \bar{c} , \bar{d} and \bar{g} appearing in (3.7) are independent of time. We emphasize, however, that many of the results that follow can be extended in a straightforward way to the more general form of the DMGLE (2.12).

Symmetries. The DMGLE (3.7) enjoys a number of symmetries. Let $u(x, t)$ be any solution of (3.7). Then $u_\epsilon(x, t)$ is also a solution of (3.7) $\forall \epsilon \in \mathbb{R}$, where:

- (i) Phase invariance: $u_\epsilon(x, t) = e^{i\epsilon} u(x, t)$. (The same symmetry applies for the NLSE, CGLE and DMNLSE.)
- (ii) Space translations: $u_\epsilon(x, t) = u(x - \epsilon, t)$. (The same symmetry applies for the NLSE, CGLE and DMNLSE.)
- (iii) Time translations. $u_\epsilon(x, t) = u(x, t - \epsilon)$. (The same symmetry applies for the DMNLSE. It also applies for the NLSE and CGLE in the case of constant coefficients. In general (2.1) is *not* invariant under time translations, however.)
- (iv) ‘Chirp’: $\hat{u}_\epsilon(k, t) = e^{i\epsilon k^2/2} \hat{u}(k, t)$ is a solution of the equation with $r(\xi)$ replaced by $r_\epsilon(\xi) = e^{i\epsilon \xi} r(\xi)$. (The name comes from the fact that quadratic variations of the pulse phase are referred to as ‘chirp’ in optics [10, 48].) This symmetry, which is the same as that for the DMNLSE [1], has no analogue for either the NLSE or the CGLE.
- (v) Galilean boosts (generalized Galilean boosts if $\bar{d}(\cdot)$ is time-dependent): if $\bar{b} = 0$,

$$u_\epsilon(x, t) = e^{i\epsilon t x - \frac{1}{2}\epsilon^2 m(t)} u(x - \epsilon m(t), t) \quad (4.1)$$

with $m(t) = \int_0^t \bar{d}(t') dt'$. (The NLSE and CGLE with varying coefficients admit a similar invariance [34]. For the DMNLSE, as well as for the NLSE and CGLE with constant coefficients, it is simply $m(t) = \bar{d} t$. For the DMGLE with $\bar{b} \neq 0$, (4.1) applies only for those solutions that can be analytically continued off the real x -axis.)

- (vi) Generalized scaling symmetry. If $u(x, t; \bar{g}, s)$ is a solution of (2.12), so is

$$u_\epsilon(x, t; \bar{g}, s) = a u(ax, a^2 t; \bar{g}/a^2, a^2 s) \quad (4.2)$$

with $a = 1 + \epsilon$ and where s is the map strength parameter, as discussed below. (The parametrization of (4.2) is chosen so that the value $\epsilon = 0$ reproduces the original solution, as in all other cases.)

These invariances will allow us in section 5 to construct a two- or three-parameter family of solutions of the DMGLE (depending on whether $\bar{b} \neq 0$ or $\bar{b} = 0$, respectively) from a single stationary solution, in a similar way as for the NLSE, DMNLSE and CGLE. As we show later, however, unlike for the NLSE and DMNLSE (and like for the CGLE) the scaling invariance does *not* generate a one-parameter family of solutions. Note also that, as a result of the chirp symmetry, the constant Ξ_o in (2.8) can be chosen arbitrarily, and does not affect the solution $q(x, t)$ of the original problem (2.1), since it simply amounts to a redefinition of $\hat{u}(k, t)$. (Proper choice of Ξ_o can be useful to make the kernels simpler, however.)

Map strength. In the statement of the scaling invariance above we used the obvious fact that the solutions of the DMGLE (2.12) depend parametrically on \bar{g} . One should realize, however, that, as for the DMNLSE, solutions of the DMGLE also depend on a parameter s called the *map strength*, which quantifies the size of the zero-mean dispersion variations. The map strength (which for two-step maps was introduced in section 3) can be formally defined for any map as the L_1 -norm of Δd (in the DMGLE as for the DMNLSE [41]), namely,

$$s = |\overline{\Delta d}| = \int_0^1 |\Delta d(\zeta)| \, d\zeta. \tag{4.3}$$

One can then obtain explicitly the dependence of the kernels $r(\xi, t)$ and $R(x', x'', t)$ on s by writing $\Delta d(\zeta)$ (and consequently $\Xi(\zeta)$ via (2.8)) in terms of normalized functions. That is, given any choice of map $\Delta d_o(\zeta)$, we can define the normalized function $\Delta d_{\text{ref}}(\zeta) = \Delta d_o(\zeta)/|\overline{\Delta d_o}|$. One can then introduce a one-parameter family of dispersion functions

$$\Delta d_s(\zeta) = s \Delta d_{\text{ref}}(\zeta). \tag{4.4}$$

In this way one can study the behaviour of solutions for different values of map strengths within the framework of the DMGLE, without needing to go back to (2.1). When necessary, we express this dependence explicitly by writing the solution of (2.12) as $u(x, t; \bar{g}, s)$, like we did in (4.2). Of course, in the limit $s \rightarrow 0$ the DMGLE (3.7) reduces to the CGLE with constant coefficients. Using the map strength parameter, it is now easy to show that, if \bar{d} , \bar{g} and K are independent of t , the generalized scaling invariance (4.2) holds. Of course this invariance reduces to those of the DMNLSE, CGLE and NLSE in the cases $s = 0$ and/or $\bar{b} = \bar{c} = \bar{g} = 0$.

Rate equations. Like the CGLE, and unlike the NLSE and DMNLSE, the DMGLE is not a Hamiltonian system. Hence it is not possible to use Noether’s theorem to derive conservation laws from the symmetries of the equation as done for the NLSE [33]. Nonetheless, by analogy with the NLSE/DMNLSE, it is still possible to associate each symmetry with a rate equation. For brevity we only list the first three such equations, and only in the special case $\bar{b} = 0$:

$$\begin{aligned} \frac{d}{dt} \int |u|^2 \, dx &= 2\bar{g} \int |u|^2 \, dx \\ &\quad - 2\bar{c} \iiint u_{(x)}^* u_{(x+x')} u_{(x+x'')} u_{(x+x'+x'')}^* R_{(x'x'')} \, dx' \, dx'' \, dx, \end{aligned} \tag{4.5a}$$

$$\begin{aligned} \frac{d}{dt} \text{Im} \int u^* \partial_x u \, dx &= 2\bar{g} \text{Im} \int u^* \partial_x u \, dx \\ &\quad - 2\bar{c} \text{Im} \int (\partial_x u^*) u_{(x+x'')} u_{(x+x''')} u_{(x+x'+x''')}^* R_{(x'x'')} \, dx' \, dx'' \, dx, \end{aligned} \tag{4.5b}$$

$$\begin{aligned} \frac{1}{2} \frac{d}{dt} \left[\bar{d} \int |\partial_x u|^2 \, dx - \iiint u_{(x)}^* u_{(x+x')} u_{(x+x'')} u_{(x+x'+x'')}^* R_{(x'x'')} \, dx' \, dx'' \, dx \right] \\ = \bar{g} \left[\bar{d} \int |\partial_x u|^2 \, dx - 2 \int u_{(x)}^* u_{(x+x')} u_{(x+x'')} u_{(x+x'+x'')}^* R_{(x'x'')} \, dx' \, dx'' \, dx \right] \\ + \bar{c} \left[\bar{d} \text{Re} \iiint (\partial_x^2 u^*) u_{(x+x')} u_{(x+x'')} u_{(x+x'+x'')}^* R_{(x'x'')} \, dx' \, dx'' \, dx \right. \\ \left. + 2 \int \left| \iiint u_{(x+x')} u_{(x+x'')} u_{(x+x'+x'')}^* R_{(x'x'')} \, dx' \, dx'' \right|^2 \, dx \right], \end{aligned} \tag{4.5c}$$

where for brevity we used the notation $\partial_x u = \partial u_{(x)}/\partial x$, etc. Each of the above rate equations reduces to those of the NLSE [33, 60], CGLE and DMNLSE in the appropriate limits, of course. (It appears however that, even in the simpler version obtained for $s = 0$, that is for the CGLE, the third rate equation is not widely known; cf [13].) In particular, for the NLSE and DMNLSE, the right-hand-side is zero, and the integrals on the left-hand side of equations (4.5a)–(4.5c), which are then the conserved quantities of the corresponding equation, are respectively the pulse energy, the momentum and the Hamiltonian. Because of the physical meaning associated with these integrals, the rate equations for the NLSE and DMNLSE have been extensively used to study the evolution of various pulse characteristics. The rate equations of the DMGLE should therefore prove to be similarly useful.

Linear modes. If $u(x, t)$ is any solution of (3.7) and $u_\epsilon(x, t) = u(x, t) + \epsilon w(x, t)$ is also a solution, then $w(x, t)$ belongs to the nullspace of the linearized DMGLE operator about $u(x, t)$. That is, solves the linearized DMGLE $L[w, u] = 0$, where (for $\bar{b} = 0$)

$$L[w, u] = i \frac{\partial w}{\partial t} + \frac{1}{2} d \frac{\partial^2 w}{\partial x^2} - i \bar{g} w + 2(1 + i\bar{c}) \iint w_{(x+x')} u_{(x+x'')} u_{(x+x'+x'')}^* R_{(x'x'')} dx' dx'' \\ + (1 + i\bar{c}) \iint u_{(x+x')} u_{(x+x'')} w_{(x+x'+x'')}^* R_{(x'x'')} dx' dx''. \quad (4.6)$$

It then follows that, for each continuous invariance of the DMGLE, there exists a solution of the linearized DMGLE in the form

$$w(x, t) = \left. \frac{\partial u_\epsilon(x, t)}{\partial \epsilon} \right|_{\epsilon=0}, \quad (4.7)$$

similarly to the CGLE, NLSE and DMNLSE [41]. Then, by simply applying the invariances listed above, we obtain the following set of linear modes and generalized linear modes:

$$w_1 = iu, \quad w_2 = -\frac{\partial u}{\partial x}, \quad w_3 = -\frac{\partial u}{\partial t}, \quad w_4 = iXu, \quad (4.8a)$$

$$w_5 = u + x \frac{\partial u}{\partial x} + 2s \frac{\partial u}{\partial s} - 2\bar{g} \frac{\partial u}{\partial \bar{g}}, \quad (4.8b)$$

corresponding, respectively, to phase rotations, space translations, Galilean boosts and scaling transformations as given above. (Of course w_4 only applies when $\bar{b} = 0$. Note also that the chirp symmetry requires changing the kernels, so the above analysis does not apply.) The above linear modes and generalized modes satisfy the relations

$$L[w_1, u] = L[w_2, u] = L[w_3, u] = 0, \quad (4.9a)$$

$$L[w_4, u] = iw_2, \quad L[w_5, u] = 2iw_3. \quad (4.9b)$$

In the special case of travelling wave solutions, time translations are simply a composition of space translations and phase rotations. As a result, for traveling wave solutions w_3 can be expressed as a linear combination of w_1 and w_2 , and is not an independent mode. This is consistent with the familiar result [60] that for the NLSE in N spatial dimensions the linearized operator around a solitary-wave solution has a zero eigenvalue of multiplicity $2N + 2$. (The result also applies to the DMNLSE [54].)

The linearized DMGLE is of course useful to study the stability of solutions. As in the NLSE and DMNLSE, the linear modes of the DMGLE generate changes in the solution parameters, and can be used to quantify the change of these parameters under perturbations [29, 41]. Because of the presence of a nontrivial nullspace, secularities arise even if all eigenvalues of L have zero or negative real part, and as a result the change in

the solution of the DMGLE does not in general remain bounded in time. As usual, secular terms are removed by taking the solution parameters to be slowly dependent on time and determining their evolution by projecting the perturbation onto the linear modes. The existence of a generalized mode corresponding to the generalized scaling invariance is then important because the coupling between amplitude and phase in the NLSE/DMNLSE is the mechanism whereby the variance of noise-induced phase perturbations grows cubically [26] (similarly to the well-known coupling between frequency and timing jitter [25]). Even though the relation between amplitude and phase is broken in the DMGLE due to the presence of gain and gain saturation, the existence of a generalized mode associated with the phase suggests that the noise-induced phase variance could still grow cubically.

5. Solutions, stability and parameter dependence

We now discuss special solutions of the DMGLE. Again, for concreteness, we restrict our consideration to the specific form of the DMGLE arising in femtosecond lasers, namely (3.7) with constant coefficients.

Soliton solutions of the DMGLE. We start by looking for stationary solutions, that is, solutions in the form

$$u(x, t) = f(x) e^{i\lambda^2 t/2}. \quad (5.1)$$

(Recall that a family of traveling wave solutions can be obtained from (5.1) by applying the invariances of the DMGLE.) Substituting the Fourier transform of the above ansatz in (3.7) yields the following nonlinear integral equation:

$$\left[\frac{1}{2}\lambda^2 + \frac{1}{2}(\bar{d} - i\bar{b})k^2 + i\bar{g} \right] \hat{f} = (1 + i\bar{c}) \iint \hat{f}_{(k+k')} \hat{f}_{(k+k'')} \hat{f}_{(k+k'+k'')}^* r_{(k'k'')} dk' dk''. \quad (5.2)$$

Although closed-form solutions are not available unless $r(\cdot) = \text{const}$, (5.2) can be efficiently integrated numerically (see appendix). Note also that, similarly to the DMNLSE [41, 44], fast numerical methods can be used for the calculation of the double integral in equations (3.7) and (5.2) and thus to solve numerically both the integral equation (5.2) and the DMGLE (3.7) itself (again, see appendix). Hence, the computational complexity of the DMGLE is no less and no greater than that of the original, un averaged equation (2.1).

Of course, solutions of (5.2) are not solitons in the mathematical sense of the term (that is, solutions corresponding to the discrete spectrum of the scattering problem associated with the given nonlinear partial differential equation [9]), but rather solitary waves. As common in physics and optics, however [10, 18, 36, 48, 65], we will refer to such a pulse as a soliton—or, in the case of the DMNLSE and DMGLE, as a dispersion-managed soliton (DMS). Importantly, while for the NLSE and the DMNLSE one can find solutions for any real λ , for the CGLE and the DMGLE nontrivial solutions exist only for *discrete* values of λ .

Figure 2 shows the real and imaginary parts of stationary solutions of the NLSE, CGLE, DMNLSE and DMGLE, while figure 3 shows the modulus of the same solutions in semi-logarithmic scale. The values of λ that yield the unique solution with the given value of the parameters for the CGLE and the DMGLE are, respectively, $\lambda_{\text{cgle}} = 3.86$ and $\lambda_{\text{dmgle}} = 4.43$, as obtained numerically using the methods described in appendix. For the NLSE and the DMNLSE, the value of λ was chosen so that the corresponding solutions have the same peak amplitude as those of the CGLE, respectively. Such values are easily obtained by noting that, for both the NLSE and DMNLSE, $\lambda = \max_{x \in \mathbb{R}} |u(x, 0)|$. In all cases, 1024 Fourier modes were used in the simulations.

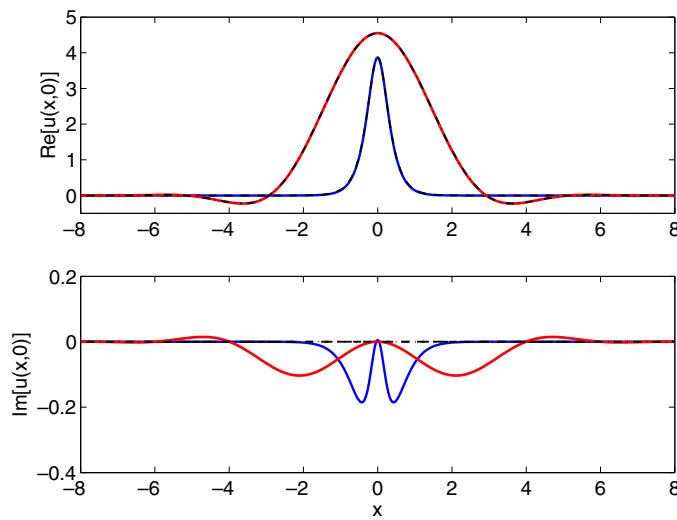


Figure 2. Shape of the solutions of (5.2). Solid (blue) line: CGLE ($s = 0$, $\bar{g} = 2$, $\bar{b} = \bar{c} = 0.2$); dashed black line: NLSE ($s = \bar{b} = \bar{c} = \bar{g} = 0$); thick solid (red) line: DMGLE ($s = 4$, $\bar{g} = 2$, $\bar{b} = \bar{c} = 0.2$); dot-dashed black line: DMNLSE ($s = 4$, $\bar{b} = \bar{c} = \bar{g} = 0$). In all cases $\bar{d} = 1$. The value of λ for the NLSE and the DMNLSE was chosen so that their solutions have the same peak amplitude as those of the CGLE and DMGLE, respectively. The imaginary part of the solutions of both the NLSE and the DMNLSE is identically zero, while the real part is almost indistinguishable from that of solutions of the CGLE and DMGLE, respectively.

It should be clear from these figures that the solutions of the DMGLE combine some features of the solutions of the CGLE with some of the solutions of the DMNLSE. For example, it is evident from both figures 2 and 3 that the shape of the soliton solutions of the DMGLE is remarkably similar to that of the soliton solutions of the DMNLSE. At the same time, however, figure 2 shows that, like the solutions of the CGLE, and unlike those of the DMNLSE, a small but nonzero imaginary component appears. As a consequence, the solutions of the DGMLE do not appear to possess zeros, unlike those of the DMNLSE.

Parameter dependence. To further explore the similarities and differences between solutions of the DMGLE, CGLE and DMNLSE, we next look at their parameter dependence. Even though the parameter λ appears in identical way in the integral equation for the solutions of the DMNLSE and DMGLE, it nonetheless plays a very different role in the two cases. To see why, we briefly look at the case $s = 0$ and compare solutions of the NLSE and the CGLE. When transformed back to the physical domain, the solutions of (5.2) are, in this case,

$$u_{\text{nlse}}(x, t) = \sqrt{\bar{d}} a \operatorname{sech}(ax) e^{ia^2 \bar{d}t/2}, \quad (5.3a)$$

$$u_{\text{cgle}}(x, t) = \sqrt{\bar{d}} [A \operatorname{sech}(\eta x)]^{1+iv} e^{i\mu \bar{d}t}, \quad (5.3b)$$

where a is an arbitrary real constant, while [11]

$$A = \sqrt{\frac{3v(1 + \bar{b}^2) \bar{g}}{\bar{c}\alpha}}, \quad \eta = \sqrt{\frac{2\bar{g}}{\alpha}}, \quad \mu = (1 - v^2 - 2v\bar{b}) \frac{\bar{g}}{\alpha},$$

with

$$\alpha = 2v - \bar{b}(1 - v^2), \quad v = \frac{-3(1 - \bar{b}\bar{c}) + \sqrt{9(1 - \bar{b}\bar{c})^2 + 8(\bar{b} + \bar{c})^2}}{2(\bar{b} + \bar{c})}. \quad (5.4)$$

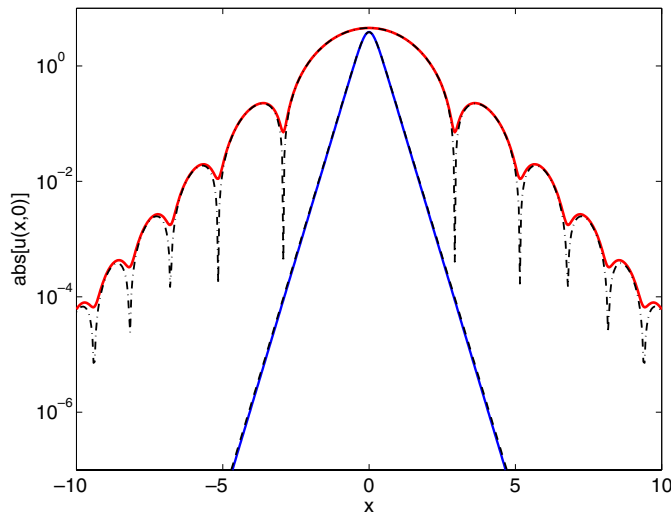


Figure 3. Absolute value of the stationary solutions in semi-logarithmic scale for the same cases as in figure 2. (Line colours and styles are also the same.) Solutions of the DMGLE have exponentially decaying oscillating tails, such as those of the DMNLSE, with the frequency of the oscillations increasing along the tails. Unlike the solutions of the DMNLSE, however, solutions of the DMGLE do not appear to possess zeros, due to the presence of a nonzero imaginary part.

The functional form of (5.3a) and (5.3b) is similar. The key difference, however, is that (5.3a) represents a one-parameter family of solutions, since a (the soliton amplitude, which is inversely proportional to the pulse width and coincides with the soliton eigenvalue in (5.2) as well as with the scaling parameter in (4.2)) can take any real value. In contrast, all parameters in (5.3b) are uniquely determined by the coefficients in the CGLE. Thus, none of them can play the role of the scaling parameter in (4.2). Instead, that role for (5.3b) is played by \sqrt{g} .

A similar situation arises for the DMNLSE and the DMGLE. Namely, for the DMNLSE the eigenvalue λ is also the soliton amplitude and the scaling parameter, and is in one-to-one correspondence with the pulse energy (even though the relation is not simply of direct proportionality as for the NLSE [41]). For the DMGLE, in contrast, the value of λ is completely determined by that of the coefficients in the DMGLE. Thus, in both the CGLE and the DMGLE, the addition of gain and loss dynamics seems to simply pick out one particular solution in the family of solutions of the corresponding conservative model (NLSE and DMNLSE, respectively), without significantly altering its form—at least for moderate values of the gain/loss parameters.

The above observations are corroborated by looking at the relation between the energy of the pulse and its root-mean-square width, defined, respectively, as

$$E = \int |u|^2 dx, \quad \tau = \sqrt{M_2/E}, \tag{5.5}$$

where

$$M_2 = \int x^2 |u|^2 dx.$$

For the solutions (5.3a) and (5.3b) of the NLSE and the CGLE, these integral quantities take on the following values:

$$E_{\text{nlse}} = 2\bar{d}a, \quad \tau_{\text{nlse}} = \pi/(\sqrt{3}a), \tag{5.6a}$$

$$E_{\text{cgle}} = 3\bar{d}\sqrt{g}\eta/\bar{c}, \quad \tau_{\text{cgle}} = \pi\sqrt{\eta/3g}, \tag{5.6b}$$

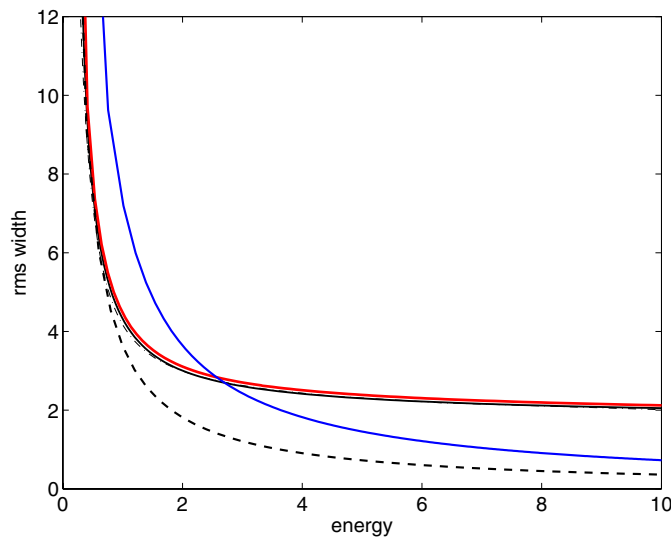


Figure 4. Root-mean-square (rms) width of the stationary solutions versus their energy for the NLSE, CGLE, DMNLSE and DMGLE (line colours and styles are as in figures 2 and 3). The data for the NLSE and the CGLE are obtained, respectively, from the first and the second of (5.7), while those for the DMNLSE and the DMGLE are obtained from numerical solution of the integral equation (5.2) for different values of λ (DMNLSE) and \bar{g} (DMGLE). The value of all the other parameters is the same as in figures 2 and 3.

with η uniquely determined from \bar{b} and \bar{c} via (5.4) as before. Eliminating a from (5.6a) and \bar{g} from (5.6b) we then obtain the well-known relations between amplitude and width, respectively, for the NLSE and the CGLE:

$$E_{\text{nlse}} \tau_{\text{nlse}} = 2\pi \bar{d} / \sqrt{3}, \quad E_{\text{cgle}} \tau_{\text{cgle}} = \sqrt{3} \pi \bar{d} \eta / \bar{c}. \quad (5.7)$$

Equivalent relations were derived in [16] for the DMNLSE using a variational approximation with a Gaussian ansatz:

$$E_{\text{dmnlse}} = \bar{d} \sqrt{\frac{\pi}{2a}} \frac{\sqrt{1+y^2}}{\{1 - \sqrt{1+y^2} \ln[(1 + \sqrt{1+y^2})/y]/2\}y}, \quad (5.8a)$$

$$\tau_{\text{dmnlse}} = \sqrt{2a}, \quad (5.8b)$$

where $y = a/s$. Eliminating a from (5.8a) and (5.8b) then yields the equivalent of (5.7). To the best of our knowledge, however, no variational approach has been developed for the CGLE that can be extended to the DMGLE. In this case, therefore, the relation between energy and width must be obtained by numerically solving the integral equation (5.2).

Figure 4 shows the rms pulse width versus its energy for the NLSE, the CGLE, the DMNLSE and the DMGLE. We see that, as a result of the dispersion management, the effects of gain dynamics are reduced compared to the constant dispersion case, and the similarity between the parameter dependence of the solutions of the DMNLSE and the DMGLE is even closer than that among the solutions of the NLSE and CGLE. (Note also that, for the DMNLSE, the data from (5.8a) and (5.8b) is almost indistinguishable from those coming from numerical solutions of (5.2).) Note however that the curves for the NLSE/DMNLSE are obtained by varying λ , while those for the CGLE/DMGLE by varying \bar{g} . Indeed, it is crucial to realize that each point in the curves for the CGLE/DMGLE is a solution of a *different* partial differential

equation. As a result the above comparison may appear to be somewhat artificial at first. In practice it is not, however. This is because solutions with different amplitude are experimentally produced by varying the pump power [57], which has precisely the effect of changing the value of the linear gain coefficient—and thus of \bar{g} —in the DMGLE (3.7).

Stability. In the absence of gain dynamics, solutions of the NLSE and one branch of solutions of the DMNLSE are stable under perturbations. In the presence of linear, band-limited gain and gain saturation, one would expect the pulse solutions of the CGLE/DMGLE to be more stable than those of the NLSE/DMNLSE. Indeed, solutions of the CGLE with constant coefficients are stable for $\alpha > 0$ [11]. (Such is the case for all the solutions in figures 2–4.) We expect that in these situations, amplitude perturbations will be damped in the DMGLE as they are in the CGLE, making the stationary pulses of the DMGLE stable. But of course this conjecture must be verified via careful analysis. One way to do so would be to perform a linearized stability analysis, that is, to look for the eigenvalues of the linearized DMGLE operator $L[w, u]$ in (4.6) when u is the solitary-wave solution (5.1) obtained via (5.2), along the lines of what was done for the DMNLSE in [17, 38, 54, 61].

6. Conclusions

In summary, we have derived the DMGLE as the equation that governs the long-term dynamics of systems described by the CGLE with time-dependent coefficients. In particular we have shown how the DMGLE arises in Ti : sapphire femtosecond lasers, we discussed the properties of the equation and of its solutions. Since the DMGLE is (like the CGLE, NLSE and DMNLSE) a universal equation, however, we believe that it will prove to be a unified model for the description many other experimental realizations of femtosecond lasers in addition to Ti : sapphire, such as similariton lasers [30], lasers using all-normal dispersion fibre [20], and those using waveguide arrays [56].

From a mathematical point of view, perhaps the most important feature of the DMGLE is that it is amenable to analytical treatment. In fact, the results of this work open up many interesting theoretical questions, as well as some important practical ones. In particular, the following are fairly natural open questions:

- Whether a proof of existence of stationary solutions is possible (as was done in [66] for the DMNLSE).
- Obtaining the asymptotic behaviour of the stationary solution as $x \rightarrow \pm\infty$ (as was done in [42, 43] for the DMNLSE).
- Whether there exist various branches of solutions as a function of \bar{d} as in the DMNLSE (e.g. see [18] and references therein).
- Whether there exist multi-pulse solutions (as in the CGLE [12] and the higher-order DMNLSE [4]).
- The stability of all of these solutions (e.g. see [54, 61] and references therein for the DMNLSE and [11, 32] for the CGLE).
- Whether there exist ‘true’ dispersion-managed solitons corresponding to the stationary solutions of the DMGLE (3.7); that is, whether there exist time-periodic solutions in the original, un averaged system (2.1). (Recall that for NLS + DM, radiative losses beyond all orders [64].)
- Even if true dispersion-managed solitons did not exist in the original, un averaged system, it should still be possible to prove that solutions of (2.1) remain $O(t_a)$ close to those of (3.7) up to times $O(1/t_a)$ (as was done for the DMNLSE [67]).

- Characterizing the large- s limit of the equation and of its solutions (as was done in [3] for the DMNLSE).
- Formulating ‘slow’ ordinary differential equations for the long-term evolution of the pulse parameters which bypass the fast dynamics inside each map (as was done in [15, 54] for the DMNLSE).
- Characterizing pulse collisions and interactions. Because neither the CGLE nor the DMNLSE [2, 37] are integrable, one would expect that the DMGLE is not either, implying that pulse interactions will be inelastic.
- More generally, since the CGLE with constant coefficients describes a remarkably rich variety of physical phenomena, including chaos [58], it will be interesting to use the DMGLE to see how these phenomena are affected by the presence of dispersion and nonlinearity management.

Since the Hamiltonian formalism is lost, however, settling these issues might be significantly more complicated than for conservative systems such as the NLSE and DMNLSE.

A more complicated equation of DMNLS type with gain and loss was also recently studied in [5] as a model for Ti : sapphire lasers. Also, a review of different mathematical approaches for the study of dispersion management in optical fibres can be found in [18]. All of the works cited in [18], however, deal with conservative systems. To the best of our knowledge, [5] and the present work are the first to generalize those tools in order to study dispersion-managed systems with significant gain dynamics.

With regard to more practical issues pertaining to Ti : sapphire femtosecond lasers, we first note that a multidimensional version of the DMGLE such as the one presented in section 2 could be useful in order to take into account the transverse dynamics of the pulses in the cavity. In any case, the DMGLE can now be used to study the sensitivity of pulses with respect to perturbations, and especially quantum noise, using the linear modes and their adjoints to guide importance-sampled Monte Carlo simulations along the line of [41, 49–51]. (For an introduction to importance sampling tailored to the study of noise in lightwave systems see [51].) Such a study will be instrumental to determine the true stability properties of pulses in these lasers and consequently to obtain the comb linewidth, which is an important step [7, 46] towards determining the ultimate accuracy of femtosecond lasers as optical atomic clocks.

Acknowledgments

I thank Mark Ablowitz, Steven Cundiff, William Kath, Curtis Menyuk, Avner Peleg and Elaine Spiller for many interesting discussions. This work was supported by NSF under grant number DMS-0506101.

Appendix: numerical methods for the DMGLE

Two relevant issues are: (i) efficient methods for numerical integration of the time-dependent DMGLE (3.7), and (ii) numerical methods to find dispersion-managed soliton solutions, i.e. solutions of the nonlinear integral equation (5.2). The first issue is rather straightforward: equation (3.7) can be integrated using essentially the same techniques as for the DMNLSE. These techniques include a method for the fast evaluation of the double integral. Since this method was discussed in detail in the appendix of [41], we do not repeat that discussion here, and we turn our attention instead to the nonlinear integral equation (5.2).

When $\bar{b} = \bar{c} = \bar{g} = 0$ (that is, for the DMNLSE), (5.2) can be efficiently solved numerically using Petviashvili’s method (as discussed in the appendix of [41]). Thus, here we

only need to address the case when \bar{b} , \bar{c} or \bar{g} are nonzero. For simplicity, we first present the method for the CGLE (that is, when $s = 0$), even though in that case one can find stationary solutions analytically. This will allow us to explain the relevant ideas—which are the same for both the CGLE and the DMGLE—without some of the notational complications resulting from the presence of the kernel $r(k'k'')$ in (5.2).

As with the DMNLSE, we solve the nonlinear integral equation (5.2) numerically by introducing an appropriate iteration scheme. Compared to the DMNLSE, however, two additional complications must be addressed:

- (i) An appropriate correction factor is necessary for convergence, since a standard Neumann iteration diverges. This issue is similar to that arising for the DMNLSE. In that case, the problem can be solved using Petviashvili’s method. That method does not converge for the CGLE/DMGLE, however, due to the presence of both a real and an imaginary component in the solution.
- (ii) The propagation constant μ is unknown *a priori*. That is, unlike the NLSE/DMNLSE, soliton solutions of the CGLE and DMGLE only exist for certain discrete values of the propagation constant, cf (5.3*b*) and (5.4). Since these values are not known in advance, in addition to looking for the functions F_r and F_i the solution method must simultaneously look for the values of μ for which (A.1) admits nontrivial solutions.

We discuss both problems below.

We seek a complex-valued function $f(x) = f_{re} + i f_{im}$ (with f_{re} and f_{im} both even functions of x) and a propagation constant $\mu = \lambda^2/2$ such that $F(k) := \mathcal{F}[f]$ satisfies (5.2), which, when $s = 0$ (that is, for the CGLE) reduces to

$$(\mu + \frac{1}{2}(\bar{d} - i\bar{b})k^2) \hat{f} + i\bar{g}\hat{f} = (1 + i\bar{c})\mathcal{F}[fff^*]. \tag{A.1}$$

Decomposing (A.1) into its real and imaginary parts yields the following two-component real system of nonlinear integral equations:

$$(\mathbf{A} + \mu \mathbf{I}) \mathbf{F} - \mathbf{C} \mathbf{N}(\mathbf{F}) = 0, \tag{A.2}$$

where

$$\mathbf{F} = \begin{pmatrix} \hat{f}_{re} \\ \hat{f}_{im} \end{pmatrix}, \quad \mathbf{N}(\mathbf{F}) = \begin{pmatrix} \mathcal{F}[f_{re}^3] + \mathcal{F}[f_{re}f_{im}^2] \\ \mathcal{F}[f_{re}^2f_{im}] + \mathcal{F}[f_{im}^3] \end{pmatrix}, \tag{A.3}$$

\mathbf{I} is the 2×2 identity matrix and

$$\mathbf{A}(k) = \begin{pmatrix} \frac{1}{2}\bar{d}k^2 & \frac{1}{2}\bar{b}k^2 - \bar{g} \\ \bar{g} - \frac{1}{2}\bar{b}k^2 & \frac{1}{2}\bar{d}k^2 \end{pmatrix}, \quad \mathbf{C} = \begin{pmatrix} 1 & -\bar{c} \\ \bar{c} & 1 \end{pmatrix}. \tag{A.4}$$

(Of course \hat{f}_{re} and \hat{f}_{im} are also both even functions of k .)

Let us first address the issue of the unknown propagation constant. Suppose that μ_o is the exact propagation constant, and $\mu = \mu_o + \Delta\mu$. Equation (A.2) then yields

$$\Delta\mu \mathbf{F} = \mathbf{C} \mathbf{N}(\mathbf{F}) - (\mathbf{A} + \mu_o \mathbf{I}) \mathbf{F}. \tag{A.5}$$

We can therefore obtain $\Delta\mu$ as

$$\Delta\mu = \frac{\langle \mathbf{F}, \mathbf{C} \mathbf{N}(\mathbf{F}) \rangle - \langle \mathbf{F}, \mathbf{A} \mathbf{F} \rangle}{\langle \mathbf{F}, \mathbf{F} \rangle} - \mu_o, \tag{A.6}$$

Here the inner product of two real vector functions is

$$\langle \mathbf{F}, \mathbf{G} \rangle = \int \mathbf{F}(k) \cdot \mathbf{G}(k) dk. \tag{A.7}$$

Of course (A.6) contains the solution \mathbf{F} , which is not known exactly during the iteration. Nonetheless, (A.6) provides a way to update our estimate of the correct eigenvalue.

We now turn to the issue of convergence factors. This problem can be dealt with using the spectral renormalization method [8]. To implement this method, we start by noting that μ is not sign-definite, and even in those cases where μ is positive, some iterations might accidentally yield a negative estimate. In order to avoid problems with zero denominators, it is therefore convenient to add and subtract the term \mathbf{F} from equation (A.2), rewriting it as

$$(\mathbf{A} + \mathbf{I})\mathbf{F} = (1 - \mu)\mathbf{F} + \mathbf{C}\mathbf{N}(\mathbf{F}). \quad (\text{A.8})$$

We then introduce the real convergence factor γ and rescale the solution as $\mathbf{F} = \gamma\mathbf{V}$. Noting that $\mathbf{N}(\mathbf{F}) = \gamma^3\mathbf{N}(\mathbf{V})$, for the new field we obtain the system

$$\mathbf{V} = (\mathbf{A} + \mathbf{I})^{-1}[(1 - \mu)\mathbf{V} + \gamma^2\mathbf{C}\mathbf{N}(\mathbf{V})], \quad (\text{A.9})$$

which provides the basis for the iteration. An equation for the convergence factor is also needed, of course. This is obtained by using (A.8) with $\mathbf{F} = \gamma\mathbf{V}$ and taking its inner product with \mathbf{V} , which yields

$$\gamma^2 = \langle \mathbf{V}, (\mathbf{A} + \mu\mathbf{I})\mathbf{V} \rangle / \langle \mathbf{V}, \mathbf{C}\mathbf{N}(\mathbf{V}) \rangle. \quad (\text{A.10})$$

Combining the two results, we can then define an iteration scheme as follows. At $n = 0$, choose an initial guess for $f_{\text{re}}^{(0)} + i f_{\text{im}}^{(0)}$ and $\mu^{(0)}$, and set $\gamma^{(0)} = 1$ and $\mathbf{V}^{(0)} = \mathbf{F}^{(0)}$. Then, at the $(n + 1)$ th step of the iteration:

1. Update the convergence factor $\gamma^{(n)}$ and the current estimate of the eigenvalue $\mu^{(n)}$ using (A.10) (with $\mathbf{V} = \mathbf{V}^{(n)}$ and $\mu = \mu^{(n)}$) and (A.6) (with $\mathbf{F} = \gamma^{(n)}\mathbf{V}^{(n)}$ and $\mu = \mu^{(n)}$).
2. Update the current estimate of the solution using (A.9) with the newly updated values for $\gamma^{(n)}$ and $\mu^{(n)}$.

At each iteration, the nonlinear terms can be computed using the fast Fourier transform (FFT), which reduces the computational cost of each step from $O(N^3)$ to $O(N^2 \log N)$, where N is the number of grid points or Fourier modes.

The method to find soliton solutions of the DMGLE works exactly in the same way as that for the CGLE above. The only difference is that the term $\mathcal{F}[fff^*]$ in the RHS of (A.1) is replaced by the double convolution integral $P[\hat{f}, \hat{f}, \hat{f}^*, r]$, where

$$P[\hat{f}_1, \hat{f}_2, \hat{f}_3^*, r] = \iint \hat{f}_1(k + k') \hat{f}_2(k + k'') \hat{f}_3^*(k + k' + k'') r(k'k'') dk' dk''.$$

The nonlinear term $\mathbf{N}(\mathbf{F})$ is modified accordingly. Apart from these changes, the method is exactly the same as for the CGLE. Moreover, as in the DMNLSE, the resulting double convolution integrals can still be computed efficiently using FFTs. As this issue was explained in detail in the appendix of [41], we do not duplicate that discussion here.

References

- [1] Ablowitz M J and Biondini G 1998 Multiscale dynamics in communication systems with strong dispersion management *Opt. Lett.* **23** 1668–70
- [2] Ablowitz M J, Biondini G and Olson E S 2001 Incomplete collisions of wavelength-division multiplexed dispersion-managed solitons *J. Opt. Soc. Am. B* **18** 577–83
- [3] Ablowitz M J, Hirooka T and Biondini G 2001 On quasi-linear dispersion-managed transmission systems *Opt. Lett.* **26** 459–61
- [4] Ablowitz M J, Hirooka T and Inoue T 2002 Higher-order asymptotic analysis of dispersion-managed transmission systems: solutions and their characteristics *J. Opt. Soc. Am. B* **19** 2876–85
- [5] Ablowitz M J, Horikis T P and Ilan B 2008 Solitons in dispersion-managed mode-locked lasers *Phys. Rev. A* **77** 33814

- [6] Ablowitz M J, Ilan B and Cundiff S T 2004 Carrier-envelope phase slip of ultrashort dispersion managed solitons *Opt. Lett.* **29** 1808–10
- [7] Ablowitz M J, Ilan B and Cundiff S T 2006 Noise-induced linewidth in frequency combs *Opt. Lett.* **29** 1875–7
- [8] Ablowitz M J and Musslimani Z H 2005 Spectral renormalization method for computing self-localized solutions to nonlinear systems *Opt. Lett.* **30** 2140–2
- [9] Ablowitz M J and Segur H 1981 *Solitons and the Inverse Scattering Transform* (PA: Society for Industrial and Applied Mathematics, Philadelphia)
- [10] Agrawal G P 2001 *Nonlinear Fiber Optics* (San Diego, CA: Academic)
- [11] Akhmediev N, Afanasjev V V and Soto-Crespo J M 1996 Singularities and special solutions of the cubic-quintic complex Ginzburg–Landau equation *Phys. Rev. E* **53** 1190–201
- [12] Akhmediev N and Ankiewicz A (ed) 2005 *Dissipative Solitons* (New York: Springer)
- [13] Akhmediev N, Ankiewicz A and Soto-Crespo J M 1997 Multisoliton solutions of the complex Ginzburg–Landau equation *Phys. Rev. Lett.* **79** 4047–50
- [14] Aranson I S and Kramer L 2002 The world of the complex Ginzburg–Landau equation *Rev. Mod. Phys.* **74** 99–143
- [15] Biondini G and Chakravarty S 2001 Nonlinear chirp of dispersion-managed return-to-zero pulses *Opt. Lett.* **26** 1761–3
- [16] Biondini G and Chakravarty S 2003 On the characteristic parameters of dispersion-managed optical pulses *Nonlinear Physics. Theory and Experiment: II* ed M J Ablowitz *et al* (Singapore: World Scientific)
- [17] Capobianco A D, Nalesso G, Tonello A, Consolandi F and De Angelis C 2003 Noise evolution and soliton internal modes in dispersion-managed fiber systems *Opt. Lett.* **28** 1754–6
- [18] Cauterarts V, Maruta A and Kodama Y 2000 On the dispersion managed soliton *Chaos* **10** 515–28
- [19] Chen Y, Kärtner F X, Morgner U, Cho S H, Haus H A, Ippen E P and Fujimoto J G 1999 Dispersion-managed mode-locking *J. Opt. Soc. Am. B* **16** 1999–2004
- [20] Chong A, Buckley J, Renninger W and Wise F 2006 All-normal-dispersion femtosecond fiber laser *Opt. Express* **14** 10095–100
- [21] Cross M C and Hohenberg P 1993 Pattern formation out of equilibrium *Rev. Mod. Phys.* **65** 851–1112
- [22] Cundiff S T and Ye J 2003 Femtosecond optical frequency combs *Rev. Mod. Phys.* **75** 325–42
- [23] Diddams S A *et al* 2001 An optical clock based on a single trapped $^{199}\text{Hg}^+$ ion *Science* **293** 825–8
- [24] Gabitov I R and Turitsyn S K 1996 Averaged pulse dynamics in a cascaded transmission system with passive dispersion compensation *Opt. Lett.* **21** 327–9
- [25] Gordon J P and Haus H A 1986 Random walk of coherently amplified solitons in optical fiber transmission *Opt. Lett.* **11** 665–7
- [26] Gordon J P and Mollenauer L F 1990 Phase noise in photonic communications systems using linear amplifiers *Opt. Lett.* **15** 1351–3
- [27] Haus H A 2000 Mode-locking of lasers *IEEE J. Sel. Top. Quantum Electron.* **6** 1173–85
- [28] Haus H A, Fujimoto J G and Ippen E P 1992 Analytic theory of additive pulse mode-locking *IEEE J. Quantum Electron.* **28** 2086–96
- [29] Iannone E, Matera F, Mecozzi A and Settembre M 1998 *Nonlinear Optical Communication Networks* (New York: Wiley)
- [30] Ö Ilday F, Buckley J R, Clark W G and Wise F W 2004 Self-similar evolution of parabolic pulses in a laser *Phys. Rev. Lett.* **92** 213902
- [31] Jones D J, Diddams S A, Ranka J K, Stentz A, Windeler R S, Hall J L and Cundiff S T 2000 Carrier-envelope phase control of femtosecond mode-locked lasers and direct optical frequency synthesis *Science* **288** 635–9
- [32] Kapitula T, Kutz J N and Sandstede B 2002 Stability of pulses in the master mode-locking equation *J. Opt. Soc. Am. B* **19** 740–6
- [33] Kath W L 1997 A modified conservation law for the phase of the nonlinear Schrödinger equation *Math. Appl. Anal.* **4** 141–55
- [34] Kaup D J, Malomed B A and Yang J 1999 Collision-induced pulse timing jitter in a wavelength-division-multiplexing system with strong dispersion management *J. Opt. Soc. Am. B* **16** 1628–35
- [35] Korytin A I, Kryachko A Y and Sergeev A M 2001 Dissipative solitons in the complex Ginzburg–Landau equation for femtosecond lasers *Radiophys. Quantum Electron.* **44** 428–42
- [36] Kutz J N 2006 Mode-locked soliton lasers *SIAM Rev.* **48** 629–78
- [37] Lakoba T I 1999 Non-integrability of equations governing pulse propagation in dispersion-managed optical fibers *Phys. Lett. A* **260** 68–77
- [38] Lakoba T I and Pelinovsky D E 2000 Persistent oscillations of scalar and vector dispersion-managed solitons *Chaos* **10** 539–50
- [39] Lega J, Moloney J V and Newell A C 1994 Swift-Hohenberg equation for lasers *Phys. Rev. Lett.* **73** 2978–81

- [40] Lega J, Moloney J V and Newell A C 1995 Universal description of laser dynamics near threshold *Phys. D: Appl. Phys.* **83** 478–98
- [41] Li J, Spiller E T and Biondini G 2007 Noise-induced perturbations of dispersion-managed solitons *Phys. Rev. A* **75** 053818
- [42] Lushnikov P M 2000 Dispersion-managed soliton in optical fibers with zero average dispersion *Opt. Lett.* **25** 1144
- [43] Lushnikov P M 2001 Dispersion-managed soliton in a strong dispersion map limit *Opt. Lett.* **26** 1535
- [44] Lushnikov P M 2002 Fully parallel algorithm for simulating dispersion-managed wavelength-division-multiplexed optical fiber systems *Opt. Lett.* **27** 939–41
- [45] Malomed B A 2005 *Soliton Management in Periodic Systems* (New York: Springer)
- [46] Menyuk C R, Wahlstrand J K, Willits J, Smith R P, Schibli T R and Cundiff S T 2007 Pulse dynamics in mode-locked lasers: relaxation oscillations and frequency pulling *Opt. Express* **15** 6677–89
- [47] Meshulach D and Silberberg Y 1998 Coherent quantum control of two-photon transitions by a femtosecond laser pulse *Nature* **396** 239–42
- [48] Mollenauer L F and Gordon J P 2006 *Solitons in Optical Fibers: Fundamentals and Applications* (New York: Academic)
- [49] Moore R O, Biondini G and Kath W L 2003 Importance sampling for noise-induced amplitude and timing jitter in soliton transmission systems *Opt. Lett.* **28** 105–7
- [50] Moore R O, Biondini G and Kath W L 2007 A method for the study of large noise-induced perturbations of nonlinear Schrödinger solitons using importance sampling *SIAM J. Appl. Math.* **67** 1418–39
- [51] Moore R O, Biondini G and Kath W L 2008 A method for the study of large noise-induced perturbations of nonlinear Schrödinger solitons using importance sampling *SIAM Rev.* **50** 523–49
- [52] Oppo G-L, D'Alessandro G and Firth W J 1991 Spatiotemporal instabilities of lasers in models reduced via center manifold techniques *Phys. Rev. A* **44** 4712–20
- [53] Pelinovsky D E 1995 Intermediate nonlinear Schrödinger equation for internal waves in a fluid of finite depth *Phys. Lett. A* **197** 401–6
- [54] Pelinovsky D E 2000 Instabilities of dispersion-managed solitons in the normal dispersion regime *Phys. Rev. E* **62** 4283–93
- [55] Pelinovsky D E, Kevrekides P G and Frantzeskakis D J 2003 Averaging for solitons with nonlinearity management *Phys. Rev. Lett.* **91** 240201
- [56] Proctor J and Kutz J N 2005 Passive mode-locking by use of waveguide arrays *Opt. Lett.* **30** 2013–5
- [57] Quraishi Q, Cundiff S T, Ilan B and Ablowitz M J 2005 Dynamics of nonlinear and dispersion managed solitons *Phys. Rev. Lett.* **94** 243904
- [58] Soto-Crespo J M and Akhmediev N 2005 Soliton as strange attractor: nonlinear synchronization and chaos *Phys. Rev. Lett.* **95** 024101
- [59] Staliunas K 1994 Laser Ginzburg–Landau equation and laser hydrodynamics *Phys. Rev. A* **48** 1573–81
- [60] Sulem C and Sulem P-L 1989 *The Nonlinear Schrödinger Equation: Self-focusing and Wave Collapse* (New York: Springer)
- [61] Tonello A, Capobianco A D, Nalesso G, Gringoli F, De Angelis C 2005 Perturbations, internal modes and noise in dispersion-managed soliton transmission *Opt. Commun.* **246** 393–403
- [62] Udem T, Holzwarth R and Hänsch T W 2002 Optical frequency metrology *Nature* **416** 233–7
- [63] Yang T-S and Kath W L 1997 Analysis of enhanced-power solitons in dispersion-managed optical fibers *Opt. Lett.* **22** 985–7
- [64] Yang T-S and Kath W L 2001 Radiation loss of dispersion-managed solitons in optical fibers *Phys. D: Appl. Phys.* **149** 80–94
- [65] Ye J and Cundiff S T (ed) 2004 *Femtosecond Optical Frequency Comb: Principle, Operation and Applications* (New York: Springer)
- [66] Zharnitsky V, Grenier E, Turitsyn S, Jones R C K T and Hesthaven J 2000 Ground states of dispersion-managed nonlinear Schrödinger equation *Phys. Rev. E* **62** 7358–64
- [67] Zharnitsky V, Grenier E, Jones R C K T and Turitsyn S K 2001 Stabilizing effects of dispersion management *Phys. D: Appl. Phys.* **152** 794–817